Notch1–STAT3–ETB$_R$ signaling axis controls reactive astrocyte proliferation after brain injury

Matthew D. LeComte[a,b,c], Issei S. Shimada[a,1], Casey Sherwin[a,b,c], and Jeffrey L. Spees[a,b,c,2]

[a]Department of Medicine, Stem Cell Core, University of Vermont, Colchester, VT 05446; [b]Department of Neurological Sciences, University of Vermont, Burlington, VT 05401; and [c]Neuroscience Graduate Program, University of Vermont, Burlington, VT 05401

Edited by Ben A. Barres, Stanford University School of Medicine, Stanford, CA, and approved June 3, 2015 (received for review January 16, 2015)

Defining the signaling network that controls reactive astrogliosis may provide novel treatment targets for patients with diverse CNS injuries and pathologies. We report that the radial glial cell antigen RC2 identifies the majority of proliferating glial fibrillary acidic protein-positive (GFAP$^+$) reactive astrocytes after stroke. These cells highly expressed endothelin receptor type B (ETB$_R$) and Jagged1, a Notch1 receptor ligand. To study signaling in adult reactive astrocytes, we developed a model based on reactive astrocyte-derived neural stem cells isolated from GFAP-CreER-Notch1 conditional knockout (cKO) mice. By loss- and gain-of-function studies and promoter activity assays, we found that Jagged1/Notch1 signaling increased ETB$_R$ expression indirectly by raising the level of phosphorylated signal transducer and activator of transcription 3 (STAT3), a previously unidentified *EDNRB* transcriptional activator. Similar to inducible transgenic GFAP-CreER-Notch1-cKO mice, GFAP-CreER-ETB$_R$-cKO mice exhibited a defect in reactive astrocyte proliferation after cerebral ischemia. Our results indicate that the Notch1–STAT3–ETB$_R$ axis connects a signaling network that promotes reactive astrocyte proliferation after brain injury.

reactive astrocyte | Notch1 | STAT3 | ETB$_R$ | proliferation

Reactive astrogliosis occurs after most forms of CNS injury, including cerebral ischemia and trauma (1). Based on the size and duration of CNS injury, astrocytes undergo dramatic changes in gene expression, morphology (hypertrophy), and proliferation (2). Proliferating reactive astrocytes perform key activities that impact tissue preservation, repair/remodeling, and functional outcome. Specific deletion of proliferating reactive astrocytes after brain injury was shown to prevent repair of the blood–brain barrier and increase immune cell infiltration and neuronal degeneration (3, 4). Similarly, specific astroglial deletion after spinal cord injury increased immune cell infiltration, demyelination, neuronal death, and motor deficit (5). Defining signaling mechanisms that control reactive astrogliosis may lead to new treatments that maintain or repair the blood–brain barrier, control immune cell infiltration, provide neuroprotection, and/or reduce or modify glial scarring (6–9). However, the signaling network that regulates reactive astrocyte proliferation and function(s) is complex and remains poorly understood.

Studies with Cre-loxP–based conditional-knockout (cKO) mouse models that target reactive astrocytes have shown that signal transducer and activator of transcription 3 (STAT3) is an important signaling component in reactive astrogliosis (10, 11). STAT3 is activated during CNS injury, and phosphorylated STAT3 (p-STAT3) transduces signals for multiple molecules secreted or released from damaged cells such as EGF and factors that bind gp130 receptor [e.g., IL-6, leukemia inhibitory factor (LIF), and cilliary neurotrophic factor]. Using inducible glial fibrillary acidic protein (GFAP)-CreER-Notch1 cKO, we reported that Notch1 signaling regulates reactive astrocyte proliferation after stroke (8).

Relative to their distance from cell/tissue damage, subpopulations of reactive astrocytes exhibit increased expression of intermediate filament proteins such as GFAP, Nestin, and a Nestin variant with posttranslational modifications detected by the RC2 monoclonal antibody (12–15). During cortical development, the RC2 antigen is expressed by proliferating radial glial cells that are regulated by Notch1 signaling (16–18). Although rarely expressed in healthy adult cortical tissue, the RC2 antigen is re-expressed by a subpopulation of proliferative reactive astrocytes early after brain injury (19).

Here we demonstrate that the majority of proliferating reactive astrocytes express RC2 antigen after stroke (hereafter called "RC2$^+$ reactive astrocytes") and report a sorting scheme for prospective isolation of RC2$^+$ reactive astrocytes directly from injured cortex based on cell-surface expression of Jagged1, a Notch1 ligand. In addition to Jagged1 and Notch1, RC2$^+$ reactive astrocytes highly expressed endothelin receptor type B (ETB$_R$). Investigating whether Notch1 signaling interacted with ETB$_R$, we found that Jagged1 increased ETB$_R$ levels in an indirect manner, through STAT3. Experiments with inducible GFAP-CreER-ETB$_R$-cKO mice demonstrated that ETB$_R$ is necessary for reactive astrocyte proliferation. Our results identify ETB$_R$ as a transcriptional target of STAT3 and demonstrate a Notch1–STAT3–ETB$_R$ signaling axis that promotes reactive astrogliosis after brain injury.

Results

RC2$^+$/ETB$_R^+$ Cells Represent the Majority of Proliferating Reactive Astrocytes Early After Stroke. To understand better the astroglial signaling and receptors that control reactive astrogliosis, we focused on the subpopulation of RC2$^+$ reactive astrocytes that form immediately adjacent to the infarct core early after cerebral ischemia (19). Studying the timing of reactive astrogliosis, we

Significance

We demonstrate a signaling axis that controls reactive astrogliosis after brain injury based on the Notch1 receptor, signal transducer and activator of transcription 3 (STAT3), and endothelin receptor type B (ETB$_R$). Knowledge of the Notch1–STAT3–ETB$_R$ signaling axis provides fundamental insight into the signaling network that regulates reactive astrocyte proliferation after brain injury. In addition, we identify the first set of markers for prospective isolation of proliferative reactive astrocytes directly from injured CNS tissue (GLAST$^+$/Jagged1^{Hi}) and describe a unique method to generate large quantities of primary adult reactive astrocytes based on redifferentiation from reactive astrocyte-derived neural stem cells. These tools provide a powerful platform to map the signaling network that controls reactive astrogliosis.

Author contributions: M.D.L. and J.L.S. designed research; M.D.L., I.S.S., C.S., and J.L.S. performed research; M.D.L., I.S.S., and J.L.S. analyzed data; and M.D.L. and J.L.S. wrote the paper.

The authors declare no conflict of interest.

This article is a PNAS Direct Submission.

Freely available online through the PNAS open access option.

[1]Present address: Department of Cell Biology, University of Texas Southwestern Medical Center, Dallas, TX 75390.

[2]To whom correspondence should be addressed. Email: jeffrey.spees@uvm.edu.

This article contains supporting information online at www.pnas.org/lookup/suppl/doi:10.1073/pnas.1501029112/-/DCSupplemental.

observed GFAP$^+$/RC2$^+$ reactive astrocytes in the peri-infarct area at 1, 3, and 14 d after distal middle artery occlusion (dMCAO) but did not detect RC2 antigen by immunohistochemistry at 30 d after stroke (i.e., within the glial scar when proliferation has subsided) (Fig. S1). At 1 d after stroke, RC2$^+$ reactive astrocytes were negative for ETB$_R$ and Ki67, a marker of cell proliferation (Fig. S2). These data indicated that RC2$^+$ cells expressed the RC2 antigen before entering the cell cycle in vivo.

At 3 d after stroke, nearly all RC2$^+$ reactive astrocytes in the cortical peri-infarct area expressed ETB$_R$ [99 ± 1% (mean ± SEM); $n = 3$] (Fig. S2), and the majority (73%) of proliferating GFAP$^+$/Ki67$^+$ reactive astrocytes coexpressed RC2 (RC2$^+$/GFAP$^+$/Ki67$^+$: 1,857 ± 321.0 cells/mm^2; RC2$^-$/GFAP$^+$/Ki67$^+$: 698.6 ± 195.0 cells/mm^2; $n = 3$) (Fig. 1*A*). Staining showed that the level of ETB$_R$ expression was markedly higher in RC2$^+$ reactive astrocytes than in distal parenchymal GFAP$^+$ cells and other cortical cell types (Fig. 1).

Notch1 Signaling Regulates the Number of RC2$^+$/ETB$_R$$^+$ Reactive Astrocytes. Tamoxifen (TM)-inducible GFAP-CreER mice express CreER under control of the 2.2-kb human GFAP promoter. At 3 d after dMCAO, TM-treated GFAP-CreER-Notch1-cKO mice exhibited a significant decrease in the number of Ki67$^+$ reactive astrocytes [GFAP$^+$ (total astroglia): corn oil (vehicle)-treated, 2,293 ± 196 cells/mm^2; TM-treated, 822 ± 19.6 cells/mm^2; RC2$^+$/GFAP$^+$: oil-treated, 2,273 ± 190 cells/mm^2; TM-treated, 775 ± 33.1 cells/mm^2; RC2$^-$/GFAP$^+$: oil-treated, 20 ± 10 cells/mm^2; TM-treated, 47.5 ± 47.5 cells/mm^2; $n = 3$] (Fig. 1*B*). To examine whether Notch1 signaling affected proliferation specifically in RC2$^+$/ETB$_R$$^+$ reactive astrocytes, we performed dMCAO surgery on GFAP-CreER-Notch1-cKO mice and performed double immunohistochemistry for RC2 and ETB$_R$. At 30 d after TM administration and 3 d after dMCAO, there was a significant reduction in the number of RC2$^+$/ETB$_R$$^+$ cells in TM-treated mice compared with corn oil-treated mice (vehicle-treated, 5,254 ± 557.5 cells/mm^2; TM-treated, 2,685 ± 60.75 cells/mm^2; $n = 3$ mice per group; $P < 0.05$) (Fig. 1*C*).

To determine if Notch signaling regulated RC2$^+$ reactive astrocytes in other models of brain injury, we counted the number of RC2$^+$ reactive astrocytes in cortical tissue 3 d after stereotaxic injection of dibenzazepine (DBZ), a Gamma secretase inhibitor (GSI) that inhibits cleavage of Notch1. In the brain-stab model, we observed significantly fewer RC2$^+$ reactive astrocytes surrounding the stab injury in DBZ-injected mice than in vehicle-injected control mice (DBZ-injected, 602.7 ± 118.1 cells/mm^2; DMSO-injected, 1,835.0 ± 209.7 cells/mm^2; $n = 3$; $P = 0.01$) (Fig. S3). Similar to RC2$^+$ reactive astrocytes in the peri-infarct area after stroke, RC2$^+$ reactive astrocytes adjacent to the stab injury also coexpressed ETB$_R$ (Fig. S3).

To investigate Notch1 signaling in RC2$^+$/ETB$_R$$^+$ reactive astrocytes further, we assayed for Jagged1, a Notch1 ligand presented on the cell surface that induces Notch1 signaling in adjacent cells. We isolated reactive astrocytes from peri-infarct tissues by magnetic-activated cell sorting (MACS) with antibodies against glutamate aspartate transporter-1 (GLAST) (20). At 3 d after stroke, FACS phenotyping of GLAST$^+$ reactive astrocytes from cortical tissues of C57BL/6J mice demonstrated that cell-surface Jagged1 expression was markedly up-regulated on cells from the ischemic ipsilateral side of the brain compared with cells from the contralateral side (Fig. 2*A* and Fig. S4). Depending on the absence or presence of injury, we observed that cortical GLAST$^+$ cells partitioned into Jagged1^{Neg} and Jagged1^{Lo} cells or into Jagged1^{Neg}, Jagged1^{Lo}, and Jagged1^{Hi} cells, respectively (Fig. 2*A*). These results demonstrated that Jagged1 levels could be used to segregate three major subpopulations of reactive astrocytes after brain injury. Because FACS-compatible antibodies for ETB$_R$ were not available, we fixed and stained cells postsort that were allowed to adhere for 24 h in culture. Notably, GLAST$^+$/Jagged1^{Neg} cells adhered initially but did not survive the 24 h of culture. GLAST$^+$/Jagged1^{Lo} and GLAST$^+$/Jagged1^{Hi} cells adhered, survived, and expressed RC2, ETB$_R$, and Nestin (Fig. 2*B*).

Differential Jagged1 expression on peri-infarct reactive astrocytes suggested that GLAST$^+$ subpopulations varied in their level of Notch1 signaling. Based on their close proximity to the infarct core and their dependence on Notch1 signaling, we hypothesized that proliferating RC2$^+$/ETB$_R$$^+$ reactive astrocytes belonged to the GLAST$^+$/Jagged1^{Hi} category of GLAST$^+$ cells isolated from the peri-infarct area. To test this idea, we pooled live cell isolates from peri-infarct cortical tissues ($n = 3$ animals per group) and used the MACS/FACS strategy to assay GLAST$^+$/Jagged1$^+$ cells from GFAP-CreER-Notch1-cKO mice. Compared with control (vehicle-treated) GFAP-CreER-Notch1-cKO mice, we observed ablation of the GLAST$^+$/Jagged1^{Hi} cell population in TM-treated GFAP-CreER-Notch1-cKO mice (Fig. 2*C*). Injured (ipsilateral) cortex from C57BL/6J mice and from vehicle-treated GFAP-CreER-Notch1-cKO mice, which ostensibly should be normal, displayed similar percentages of GLAST$^+$/Jagged1^{Hi} cells [C57BL/6J: 6.89%; GFAP-CreER-Notch1-cKO (vehicle-treated): 8.37%] (Fig. S4). These results suggested that Jagged1/Notch1 signaling could occur between adjacent astrocytes to promote astroglial proliferation and potentially interact with

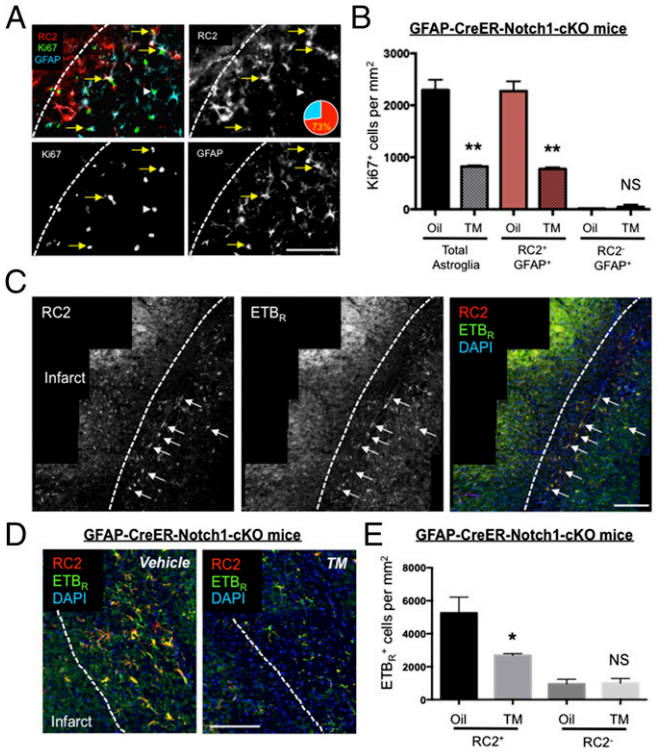

Fig. 1. RC2 marks Notch1-dependent reactive astrocytes that proliferate after injury and express high levels of ETB$_R$. (*A*) At 3 d after dMCAO, the majority of GFAP$^+$/Ki67$^+$ reactive astrocytes surrounding the infarct core expressed RC2 antigen (73%), whereas a minority of astrocytes coexpressed Ki67 and GFAP but not RC2 (white arrowhead). (*B*) cKO of Notch1 during stroke significantly reduced the number of proliferating GFAP$^+$ cells (Total astroglia) and RC2$^+$/GFAP$^+$ reactive astrocytes but not RC2$^-$/GFAP$^+$ astrocytes 3 d after stroke. $^{**}P < 0.01$; $n = 3$. NS, not significant. (*C*) RC2$^+$ astrocytes expressed high levels of ETB$_R$ (white arrows) relative to distal astrocytes and other cell types. (*D* and *E*) Conditional deletion of astroglial Notch1 in GFAP-CreER-Notch1-cKO mice significantly decreased RC2$^+$/ETB$_R$$^+$ astrocytes but not RC2$^-$/ETB$_R$$^+$ cells in the peri-infarct area 3 d after dMCAO. $^*P < 0.05$, $n = 3$. (Scale bars, 50 μm.) The three panels in (*C*) were montaged by software from multiple images in order to show a larger cortical field.

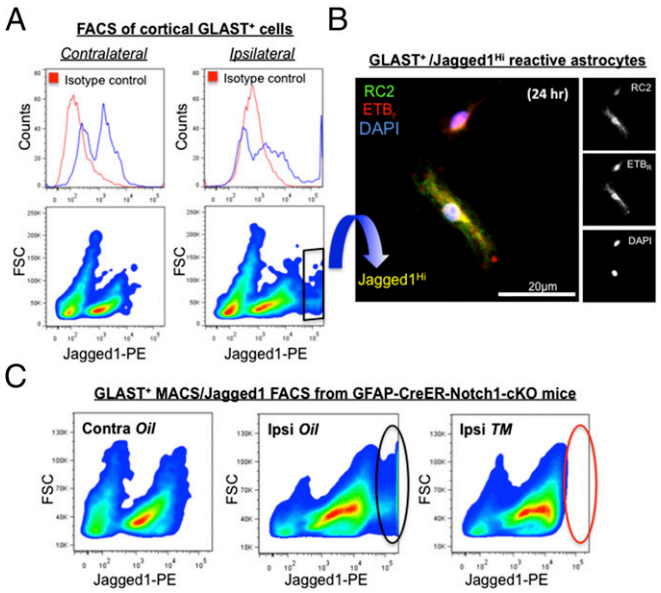

Fig. 2. Cell-surface Jagged1 levels identify distinct subpopulations of GLAST$^+$ reactive astrocytes after cortical injury. (*A*) Jagged1 phenotype of GLAST$^+$ cells isolated by MACS from pooled contralateral and ipsilateral cortical tissues of C57BL/6J mice 3 d after ischemic injury ($n = 4$ mice; ipsi- and contralateral tissues were dissected from the same animals). (*Left*) Contralateral GLAST$^+$ cells divide into two populations, Jagged1^{Neg} and Jagged1^{Lo}. For specific anti-Jagged1 stain (see area under blue line on the histogram), note the bimodal distribution indicating two populations, and that the signal from cells stained with nonspecific antibody (isotype control, area under red line) overlaps the first half of the distribution defined by the blue line (i.e., Jagged1^{Neg} cells). (*Right*) Cell-surface Jagged1 levels increase markedly on a portion of ipsilateral GLAST$^+$ cells after stroke, forming a third additional cell population (i.e., Jagged1^{Hi} cells) with a signal intensity above 10^5 (see distribution under blue line towards the far end of the histogram). (*Right, Bottom*) Isolation of Jagged1^{Hi} cells by FACS (the black rhombus indicates the gate). (*B*) Post-FACS, Jagged1^{Hi} cells adhered and were cultured for 24 h and then were fixed and stained for RC2 (green) and ETB$_R$ (red). Cell nuclei were stained by DAPI (blue). (*C*) GFAP-CreER-Notch1-cKO mice were treated with vehicle (corn oil) or TM ($n = 3$ mice per treatment group, pooled by ipsi- or contralateral cortical tissue). (*Left*) GLAST$^+$ cells isolated from contralateral cortices of oil-treated GFAP-CreER-Notch1-cKO mice lacked the population of Jagged1^{Hi} cells, similar to C57BL/6J control animals (compare with phenotype in *A*, *Lower Left*). (*Center*) Similar to ipsilateral cortices of typical C57BL/6J mice 3 d after dMCAO, a population of GLAST$^+$/Jagged1^{Hi} cells (black oval) was observed for GFAP-CreER-Notch1-cKO mice treated with oil (compare with phenotype in *A*, *Lower Right*). (*Right*) Astroglial deletion of Notch1 in TM-treated GFAP-CreER-Notch1-cKO mice largely removed the GLAST$^+$/Jagged1^{Hi} cell population (red oval). Note: Each of the three FACS phenotypes in *C* represents 4.06×10^5 cells.

ETB$_R$-based signaling in RC2$^+$/ETB$_R^+$ reactive astrocytes. The data also indicated that proliferating RC2$^+$/ETB$_R^+$ reactive astrocytes belonged to the GLAST$^+$/Jagged1^{Hi} subpopulation.

Immobilized Jagged1 Induces ETB$_R$ and Promotes Reactive Astrocyte Proliferation. Although there is a conventional method for isolating and culturing astrocytes from neonatal mice, primary adult cortical reactive astrocytes survive poorly in culture. We recently reported the isolation and expansion of self-renewing, multipotent reactive astrocyte-derived neural stem cells (Rad-NSCs) derived from the cortical peri-infarct area after stroke (20). To avoid possible differences between neonatal and adult astrocytes, we developed methods to study signaling in adult astrocytes based on redifferentiated Rad-NSCs. After redifferentiation of Rad-NSCs in medium containing 10% FCS for 7 d, we obtained cultures that were 80% GFAP$^+$/Tuj1$^-$ astrocytes (GFAP$^+$: 82 ± 5.3%; Tuj1$^+$: 7 ± 2.2%) (Fig. S5*A*). For clarity, we hereafter refer to the Rad-NSC–derived astrocytes as "Astro$^{Rad\text{-}NSC}$." When maintained in serum-containing medium, most Astro$^{Rad\text{-}NSC}$ expressed Nestin, and a few expressed the RC2 antigen (Fig. S5*B*). The above results suggested that Astro$^{Rad\text{-}NSC}$ might be used to model reactive astrocyte signaling after brain injury.

Jagged1/Notch1 signaling requires mechanical tension between Jagged1 and Notch1, which interact between adjacent cell membranes. To promote Jagged1/Notch1 signaling, we plated Astro$^{Rad\text{-}NSC}$ onto immobilized Jagged1. After 48 h, immobilized Jagged1 dramatically increased the number of RC2$^+$/Ki67$^+$ reactive astrocytes (Fig. S5*C*). To test whether exposure to Jagged1 could alter expression of ETB$_R$, we plated Astro$^{Rad\text{-}NSC}$ and postnatal day 2 (PND 2) astrocytes onto immobilized Jagged1; doing so markedly increased the level of ETB$_R$ for both Astro$^{Rad\text{-}NSC}$ (Fig. S5*D*) and PND 2 astrocytes (Fig. S5*E*).

Regulation of Promoter Activity of the Gene Expressing ETB$_R$. To investigate whether Notch intracellular domain 1 (NICD1)-mediated signaling might influence ETB$_R$ levels directly through enhanced transcription of the gene expressing ETB$_R$ (*EDNRB*), we analyzed the *EDNRB* promoter DNA sequence. NICD1 does not bind DNA directly and instead alters gene transcription by interacting with a DNA-binding transcription factor called CSL (CBF-1, suppressor of hairless, LAG-1). By promoter mapping, we did not find CSL DNA binding sequences within 10 kb of the ETB$_R$ coding sequence, indicating that the *EDNRB* promoter may not be regulated directly by NICD1. In contrast, we located multiple consensus sequences for STAT3 in human and murine *EDNRB* promoter regions that satisfied the TTM(N)$_3$DAA (D: A, G, or T; M: A or C; N: A, G, T or C) motif (21) or the TTC(N)$_4$GAA motif (22) (Fig. 3*A* and Table S1). To test for transcriptional regulation by STAT3, a pGL4 luciferase reporter vector containing the human *EDNRB* promoter sequence (−3,022 bp to +160 bp) was transfected into HEK 293 cells (23). We found that incubation of HEK 293 cells in IL-6 or LIF, cytokines that bind gp130 and signal through STAT3, led to a significant increase in *EDNRB* promoter activity ($F = 8.51$; $n = 3$; $P = 0.0002$; ANOVA) (Fig. 3*B*). Notably, this effect also occurred after the exposure of cells to EGF, which signals through EGF receptor (EGFR)/JAK2/STAT3 but not via gp130/JAK2/STAT3 (Fig. 3*B*). Next, we incubated the HEK 293 cells in IL-6, LIF, or EGF with the addition of STATTIC, a STAT3-specific pharmacological inhibitor that destabilizes p-STAT3 and prevents STAT3-mediated effects. In all cases, we observed that STATTIC attenuated the induction of *EDNRB* promoter activity that would be expected to occur after cytokine/growth factor incubation (Fig. 3*B*, *Left*). In some cases, a decrease in cell number resulting from inhibitor toxicity may appear to represent a reduction in promoter activity. As a control, we assayed cell viability on replicate plates under similar conditions of cytokine treatment and STATTIC. By assay of cellular metabolism using MTS (3-[4,5-dimethylthiazol-2-yl]-5-[3-carboxymethoxyphenyl]-2-[4-sulfophenyl]-2H-tetrazolium), treatment of HEK 293 cells with STATTIC was minimally cytotoxic (Fig. 3*B*, *Right*).

***EDNRB* Promoter Activity Is Enhanced by Coincident NICD1/p-STAT3 Signaling.** Hes1 and Hes5, transcription factors that act downstream of Notch1 signaling, were shown to stabilize JAK2 and STAT3 complex formation, thereby increasing the level of p-STAT3 during glial development (24). Kamakura et al. (24) showed that STAT3 activity is critical for Notch-induced differentiation of embryonic radial glial cells and astrocytes. To determine if Notch1 signaling altered *EDNRB* transcription by enhancing STAT3 activity, we cotransfected NICD1 expression vector with pGL4-*EDNRB* promoter/Luc reporter. Acknowledging that HEK 293 cells could differ from glial cells, we performed additional studies with an astrocytoma cell line derived from malignant human glioma (U87 cells; ATCC no. 4TB-14). By immunoblotting, U87 cells expressed low but detectable

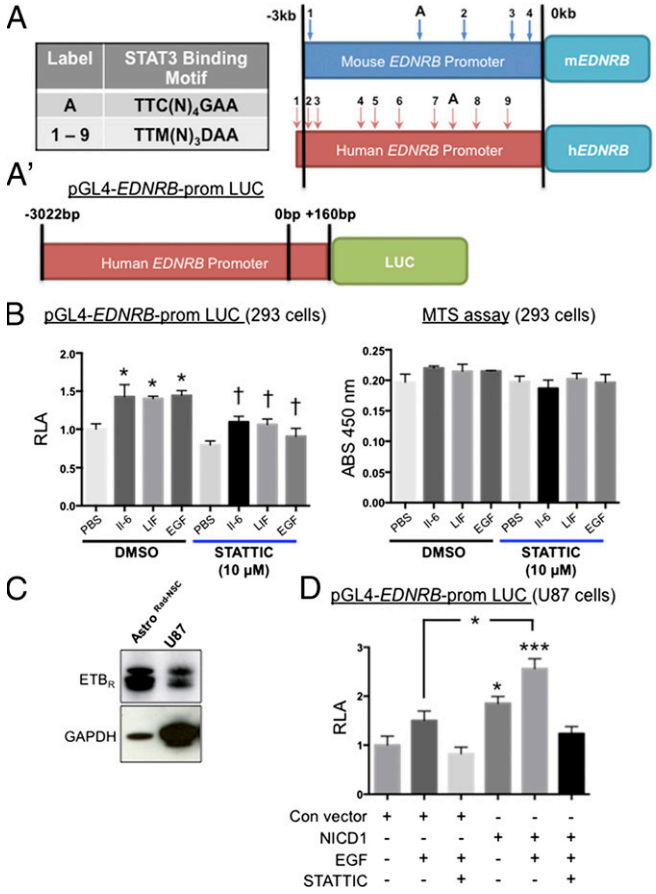

Fig. 3. Transcriptional activity at the human *EDNRB* promoter is increased by NICD1 in a STAT3-dependent manner. (*A*) Mouse and human promoter sequences of the *EDNRB* gene contain multiple putative STAT3-binding sites. The schematic indicates the relative positions of sites (arrows with labels) upstream of the transcriptional start site (0 kb) that match the STAT3-binding motif TTM(N)$_3$DAA (D: A, G, or T; M: A or C; N: A, G, T or C) (numbered 1 through 9) or motif TTC(N)$_4$GAA (N: A, G, T or C) (labeled "A"). (Table S1.) (*A'*) Schematic of the reporter construct for the human *EDNRB* promoter (pGL4-h*EDNRB*-prom) used for transfection experiments and luciferase activity assays. A 3.5-kb span of the h*EDNRB* promoter was cloned upstream of the firefly luciferase gene (LUC). +160 bp indicates the position of the start codon. (*B*, *Left*) Relative luciferase activity (RLA) of HEK 293 cells transfected with pGL4-h*EDNRB*-promoter. After 3 h of incubation in IL-6 (50 ng/mL), LIF (20 ng/mL), or EGF (20 ng/mL), luciferase activity increased significantly relative to control (PBS/DMSO). STATTIC, a specific STAT3 inhibitor, abrogated these effects. Data are shown as mean ± SEM. $*P < 0.05$ vs. DMSO/PBS; $^{\dagger}P < 0.05$ vs. relevant DMSO/growth factor or DMSO/cytokine; ANOVA; $n = 3$. (*Right*) STATTIC did not affect cell viability (MTS assay). (*C*) Expression of ETB$_R$ by Astro$^{Rad\text{-}NSC}$ and the human U87 cell line. (*D*) Compared with U87 cells transfected with control vector, U87 cells transfected with NICD1 significantly increased RLA. However, this increase was not seen in NICD1-transfected cells incubated in EGF with STATTIC or with STATTIC alone. Data are shown as mean ± SEM. $*P < 0.05$, $***P < 0.001$; ANOVA; $n = 3$.

levels of ETB$_R$ relative to Astro$^{Rad\text{-}NSC}$ (Fig. 3*C*). In the presence of EGF, U87 cells transfected with pGL4-*EDNRB* promoter/Luc reporter exhibited *EDNRB* promoter activity that was enhanced by cotransfection with NICD1 expression plasmid ($F = 14.71$; $n = 3$; $P = 0.0001$; ANOVA) (Fig. 3*D*). Notably, the action of EGF and EGF/NICD1 on *EDNRB* promoter activity in U87 cells was attenuated in the presence of STATTIC (Fig. 3*D*). These data indicated that Notch1 signaling (NICD1) could enhance STAT3 activity, perhaps by stabilizing p-STAT3 as shown by Kamakura et al. (24).

Notch1 Signaling Stabilizes/Increases p-STAT Levels in Adult Reactive Astrocytes. To examine whether increased phosphorylation of STAT3 in adult reactive astrocytes could induce ETB$_R$ expression, we incubated Astro$^{Rad\text{-}NSC}$ in medium supplemented with IL-6. As expected, exposure of adult reactive astrocytes to IL-6 increased the level of p-STAT3 ($P < 0.05$) and also GFAP, a protein regulated at the transcriptional level by STAT3 (Fig. 4*A*). Of interest, we also observed an increase in ETB$_R$ levels ($P < 0.01$) (Fig. 4*A*). To determine whether Notch1 stabilized STAT3 signaling or promoted STAT3 activation, we performed a loss-of-function experiment by treating Astro$^{Rad\text{-}NSC}$ from GFAP-CreER-Notch1-cKO mice with 4-OH-TM (hereafter OHTM) to remove Notch1 and blotted for p-STAT3. To test another factor known to stimulate gp130/JAK2/STAT3 signaling, we incubated cells with LIF. With the addition of LIF, we observed reduced NICD1 and p-STAT3 levels after 5–8 d of OHTM treatment compared with vehicle treatment ($P < 0.05$) (Fig. 4*B*).

Jagged1/Notch1 Signaling Controls the Level of ETB$_R$. To test for effects of Notch signaling on ETB$_R$, we exposed Astro$^{Rad\text{-}NSC}$ to a GSI. By real-time quantitative RT- PCR (qRT-PCR) assays,

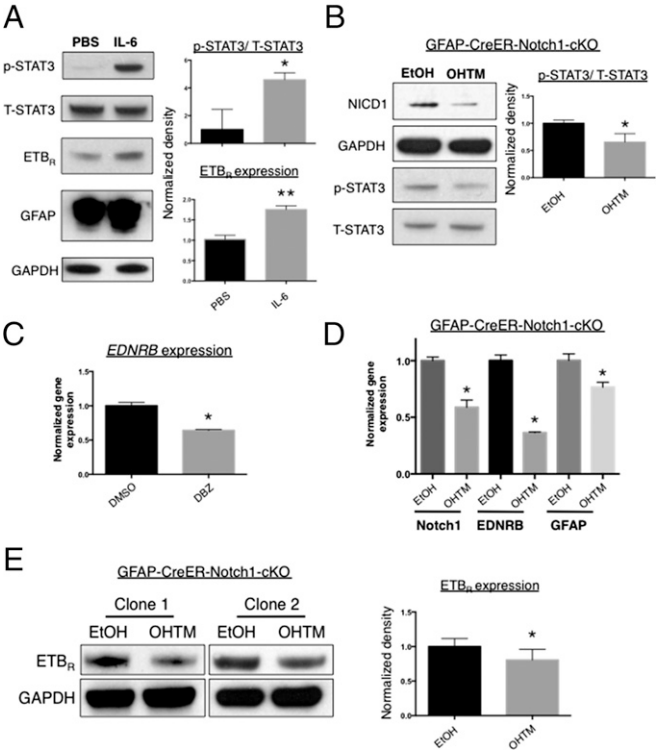

Fig. 4. Astroglial ETB$_R$ levels change in a manner correlated with STAT3 activation and are modified by the presence/absence of Notch1. (*A*) Incubation of Astro$^{Rad\text{-}NSC}$ in IL-6 (50 ng/mL) for 2 d increased the level of activated p-STAT3, ETB$_R$, and GFAP protein. $n = 3$. (*B*) Astro$^{Rad\text{-}NSC}$ generated from Rad-NSC of GFAP-CreER-Notch1-cKO mice exhibited decreased cleavage of NICD1 after exposure to OHTM for 8 d in comparison with control cells treated with vehicle (ethanol, EtOH). $n = 3$. (*C*) LIF (20 ng/mL)-induced p-STAT3 levels were reduced in Astro$^{Rad\text{-}NSC}$ after conditional deletion of Notch1. (*Left*) Immunoblot. (*Right*) Normalized band densities from immunoblot [ratio of p-STAT3 to T-STAT3]). $n = 3$. (C) Compared with vehicle (DMSO) treatment, exposure to a GSI (DBZ) for 24 h decreased *EDNRB* gene expression in Astro$^{Rad\text{-}NSC}$. Data are shown as mean ± SEM. $*P < 0.001$; unpaired *t* test; $n = 3$. (*D*) Notch1 cKO significantly reduced *EDNRB* expression in Astro$^{Rad\text{-}NSC}$. Data are shown as mean ± SEM. $*P < 0.01$; ANOVA; $n = 3$. (*E*) Astro$^{Rad\text{-}NSC}$ differentiated from different clonal Rad-NSC lines had decreased levels of ETB$_R$ after Notch1 cKO. $n = 5$. Note: Rad-NSC clones 1 and 2 were isolated from separate GFAP-CreER-Notch1-cKO animals. $*P < 0.05$, $**P < 0.01$.

incubation of reactive astrocytes in DBZ significantly reduced *EDNRB* transcription (Fig. 4*C*). To evaluate the effects of Notch1 signaling on ETB_R in adult reactive astrocytes more specifically, we produced $Astro^{Rad\text{-}NSC}$ using clonal Rad-NSCs isolated from the peri-infarct areas of GFAP-CreER-Notch1-cKO mice (20). By gene-expression assays, treatment of GFAP-CreER-Notch1-cKO reactive astrocytes with OHTM reduced mRNA for ETB_R and GFAP; this reduction was coincident with a decrease in NICD1 transcript levels (Fig. 4*D*). Furthermore, OHTM treatment of GFAP-CreER-Notch1-cKO reactive astrocytes also significantly reduced ETB_R protein expression (Fig. 4*E*).

ETB_R Controls Reactive Astrocyte Proliferation in Vivo After Stroke. To examine the role of ETB_R in the proliferation and/or function of reactive astrocytes, we generated GFAP-CreER-ETB_R-cKO mice (Fig. S6). To determine if ETB_R cKO affected reactive astrocytes, we obtained stereological counts from the peri-infarct area for the number of $GFAP^+/ETB_R^+$ cells 30 d after TM administration and 3 d after dMCAO. The number of $GFAP^+/ETB_R^+$ cells decreased significantly in TM-treated GFAP-CreER-ETB_R-cKO mice compared with vehicle-treated control mice (vehicle-treated: 6,703 ± 447.5 cells/mm^2; TM-treated: 4,233 ± 460.4 cells/mm^2; $n = 3$ mice per group; $P = 0.018$) (Fig. 5 *A* and *B*). Of interest, we found no difference in the number of $RC2^-/GFAP^+$ cells in TM- and vehicle-treated GFAP-CreER-ETB_R-cKO mice (vehicle-treated: 1,552 ± 176.1 cells/mm^2; TM-treated: 1,743 ± 410.4 cells/mm^2; $n = 5$ mice per group; $P < 0.05$) (Fig. 5*C*). However, TM treatment led to significantly reduced numbers of $RC2^+/GFAP^+$ cells relative to vehicle-treated controls (vehicle-treated: 3,318 ± 372.6 cells/mm^2; TM-treated: 1,335 ± 353.0 cells/mm^2; $n = 5$ mice per group; $P = 0.01$) (Fig. 5*C*).

Astroglial-specific deletion of ETB_R before injury decreased the number of proliferating $Ki67^+/GFAP^+$ reactive astrocytes at 30 d after TM administration and 3 d after injury (vehicle-treated: 2,504 ± 288.9 cells/mm^2; TM-treated: 829.9 ± 111.7 cells/mm^2; $n = 5$ mice per group; $P < 0.01$) (Fig. 5 *D* and *E*). By triple immunohistochemistry, we observed a significant decrease in $RC2^+/Ki67^+/GFAP^+$ reactive astrocytes in GFAP-CreER-ETB_R-cKO mice at 3 d after dMCAO (vehicle-treated: 1,896 ± 193.4 cells/mm^2; TM-treated: 388.2 ± 115.8 cells/mm^2; $n = 5$ mice per group; $P < 0.01$) (Fig. 5*D*). However, the loss of ETB_R did not affect the number of $RC2^-/Ki67^+/GFAP^+$ reactive astrocytes, highlighting the importance of ETB_R-based signaling for $RC2^+$ reactive astrocytes localized in close proximity to the cortical injury (vehicle-treated: 607.1 ± 125.4 cells/mm^2; TM-treated: 441.7 ± 79.60 cells/mm^2; $n = 5$ mice per group; $P < 0.05$) (Fig. 5*D*). Consistent with the control of reactive astrogliosis in vivo by Notch1–STAT3–ETB_R signaling, we observed a significant reduction in reactive astrocyte proliferation in GFAP-CreER-ETB_R-cKO mice that phenocopied the reduced reactive astrocyte proliferation observed in GFAP-CreER-Notch1-cKO mice after stroke (8).

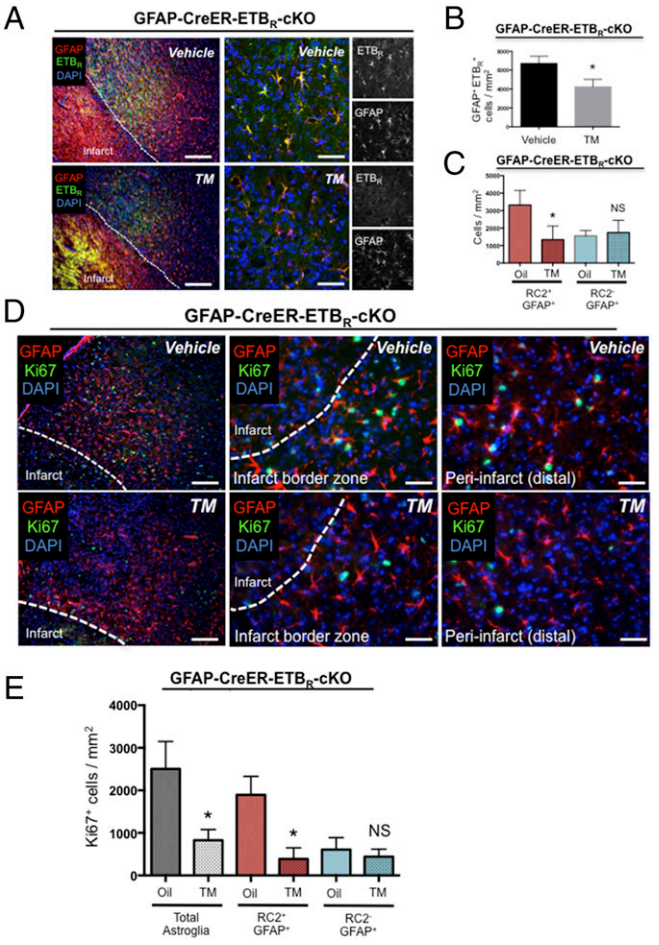

Fig. 5. ETB_R cKO depletes proliferative astrocytes in the peri-infarct area 3 d after stroke. (*A*) ETB_R cKO significantly decreased the number of $GFAP^+/ETB_R^+$ reactive astrocytes in the peri-infarct area 3 d after stroke. Note: Bright staining in infarct zone (*A*, *Left*) is autofluorescence/nonspecific background. Staining of cKO phenotype shows specificity of ETB_R antisera. (Scale bars, 200 μm.) (*B*) Quantification of $GFAP^+/ETB_R^+$ reactive astrocytes from tissue sections of brains with or without ETB_R cKO. Data are shown as mean ± SEM. $^*P < 0.05$; unpaired *t* test; $n = 3$ mice per group. (*C*) $GFAP^+/RC2^+$ reactive astrocytes, which are the majority of proliferating reactive astrocytes 3 d following stroke, were significantly decreased by ETB_R cKO. In contrast, $GFAP^+$ astrocytes negative for RC2 expression were not reduced in number. Data are mean ± SEM. $^*P < 0.01$; ANOVA with Bonferroni; $n = 5$ mice per group. NS, not significant. (*D*) ETB_R cKO reduced the number of actively dividing reactive astrocytes ($Ki67^+$) 3 d after stroke. (*Left*) Representative low-magnification images from oil-treated and TM-treated GFAP-CreER-ETB_R-cKO mice. (Scale bars, 100 μm.) (*Center*) Representative images of proximal peri-infarct area. (Scale bars, 30 μm.) (*Right*) Representative images of distal peri-infarct area. (Scale bars, 30 μm.) (*E*) ETB_R cKO significantly reduced the number of proliferating reactive astrocytes in the peri-infarct area. Note: $RC2^+/GFAP^+/Ki67^+$ (triple-positive) reactive astrocytes were significantly reduced in number within the peri-infarct area, whereas the number of $RC2^-/GFAP^+/Ki67^+$ reactive astrocytes was not affected. Data are shown as mean ± SEM. $^*P < 0.01$; ANOVA; $n = 5$ mice per group. NS, not significant.

Discussion

After CNS injury, gene transcription increases for numerous proteins that control reactive astrocyte formation and function(s) (25, 26). For GFAP, signaling through Notch1, EGFR and/or gp130 drives gene transcription directly via canonical Notch (CSL)-binding promoter elements and STAT3-binding *cis* elements (27). In contrast, we found Jagged1/Notch1 signaling could promote ETB_R expression indirectly by increasing p-STAT3. Importantly, most CNS injuries result in the local release of ET-1– and ETB_R-mediated signaling as well as the secretion of growth factors/cytokines with signals transduced by STAT3 (28). After brain injury, ET-1, EGF, and IL-6 are released by several different cell types, including reactive astrocytes, and act in an autocrine/paracrine manner (29). ET-1 signaling through ETB_R promotes the proliferation of primary astrocytes and glioblastoma cell lines (30–32), and pharmacological inhibition of ETB_R was shown to reduce reactive astrocyte proliferation in vivo after brain-stab injury and lysolecithin-induced focal demyelination (33, 34).

Gene- and protein-expression patterns can differ among populations of reactive astrocytes in response to CNS injury (25, 26, 35). Here we identified a simple epitope profile ($GLAST^+/Jagged1^+$) for prospective isolation of three different reactive astrocyte subpopulations directly from injured cortical tissue. Of

special interest, GLAST^{+}/Jagged1^{Hi} cells corresponded to the subset of RC2^{+}/Nestin^{+}/ETB$_R^{+}$ reactive astrocytes found closest to the infarct core after stroke; these cells required Notch1 and ETB$_R$ for proliferation. Previously, Notch1 signaling was reported to stabilize p-STAT3 in both normal and transformed cells (24, 36), and blockade of Notch1 signaling by GSI reduced stem-like glioblastoma cells and tumor growth in xenografts, prolonging host survival (37). Autocrine ETB$_R$ signaling is critical for self-renewal and survival of glioblastoma stem cells (tumor-initiating cells) (38), and pharmacological antagonists of ETB$_R$ decreased proliferation and survival of glioma and oligodendroglioma cells (31, 39). Our data from adult reactive astrocytes, neonatal astrocytes, HEK 293 cells, and U87 cells indicate the Notch1–STAT3–ETB$_R$ signaling axis may regulate numerous cell types that proliferate after tissue injury or transformation.

Materials and Methods

Detailed information for genotyping, dMCAO surgery, brain-stab injury, immunohistochemistry, immunocytochemistry, cell counting, Rad-NSC protocols, immunoblotting, real-time qRT-PCR, DNA constructs, and promoter activity assays is provided in *SI Materials and Methods*.

Mice. All animal work was approved by the University of Vermont College of Medicine's Office of Animal Care in accordance with the American Association for Accreditation of Laboratory Animal Care and National Institutes of Health guidelines (40). Adult male C57BL/6J mice (6–8 wk of age) were obtained from Taconic Farms. We obtained GFAP-CreER mice from Suzanne Baker, St. Jude Children's Research Hospital, Memphis, TN (41). Notch1^{tm2Rko}/GridJ mice (Notch1-flox mice; catalog no. 006951) and B6; 129-*Ednrb*^{tm1Nat}/J (EDNRB-flox mice; catalog no. 011080) were from JAX.

dMCAO Surgery. Mice were anesthetized with isoflurane (1–5%; Webster Veterinary), and body temperature was maintained with a heated pad. Focal cerebral ischemia was produced by permanently occluding the middle cerebral artery (MCA) (8, 19, 20).

Statistical Analysis. Statistical analyses were performed with GraphPad Prism software (version 6.0e). Individual groups were compared by Student's *t* test (unpaired). Multiple comparisons were made by ANOVA with Bonferroni post hoc testing. *P* values of less than 0.05 were considered significant.

ACKNOWLEDGMENTS. We thank Kazuhisa Takeda, MD, PhD (Tohoku University School of Medicine) for providing pGL3 vector containing *EDNRB* promoter DNA; Roxana del Rio-Guerra, PhD, (Harry Hood Bassett Flow Cytometry and Cell Sorting Facility at the University of Vermont) for assistance with FACS; Thomas Jetton, PhD, and William Tharp, MD, PhD, for assistance with microscopy and real-time qRT-PCR; Alexander Aronshtam, PhD, for technical support; and Krithika Rao, MS, for critical reading of the manuscript. This work was supported by National Institutes of Health Grant R01NS073815 (to J.L.S.). I.S.S. was supported by a postdoctoral fellowship from the American Heart Association, Grant 10POST3730026.

1. Pekny M, Nilsson M (2005) Astrocyte activation and reactive gliosis. *Glia* 50(4): 427–434.
2. Ridet JL, Malhotra SK, Privat A, Gage FH (1997) Reactive astrocytes: Cellular and molecular cues to biological function. *Trends Neurosci* 20(12):570–577.
3. Bush TG, et al. (1999) Leukocyte infiltration, neuronal degeneration, and neurite outgrowth after ablation of scar-forming, reactive astrocytes in adult transgenic mice. *Neuron* 23(2):297–308.
4. Myer DJ, Gurkoff GG, Lee SM, Hovda DA, Sofroniew MV (2006) Essential protective roles of reactive astrocytes in traumatic brain injury. *Brain* 129(Pt 10):2761–2772.
5. Faulkner JR, et al. (2004) Reactive astrocytes protect tissue and preserve function after spinal cord injury. *J Neurosci* 24(9):2143–2155.
6. Sofroniew MV (2009) Molecular dissection of reactive astrogliosis and glial scar formation. *Trends Neurosci* 32(12):638–647.
7. Voskuhl RR, et al. (2009) Reactive astrocytes form scar-like perivascular barriers to leukocytes during adaptive immune inflammation of the CNS. *J Neurosci* 29(37): 11511–11522.
8. Shimada IS, Borders A, Aronshtam A, Spees JL (2011) Proliferating reactive astrocytes are regulated by Notch-1 in the peri-infarct area after stroke. *Stroke* 42(11): 3231–3237.
9. Wanner IB, et al. (2013) Glial scar borders are formed by newly proliferated, elongated astrocytes that interact to corral inflammatory and fibrotic cells via STAT3-dependent mechanisms after spinal cord injury. *J Neurosci* 33(31):12870–12886.
10. Okada S, et al. (2006) Conditional ablation of Stat3 or Socs3 discloses a dual role for reactive astrocytes after spinal cord injury. *Nat Med* 12(7):829–834.
11. Herrmann JE, et al. (2008) STAT3 is a critical regulator of astrogliosis and scar formation after spinal cord injury. *J Neurosci* 28(28):7231–7243.
12. Li Y, Chopp M (1999) Temporal profile of nestin expression after focal cerebral ischemia in adult rat. *Brain Res* 838(1-2):1–10.
13. Chen Y, Swanson RA (2003) Astrocytes and brain injury. *J Cereb Blood Flow Metab* 23(2):137–149.
14. Bani-Yaghoub M, et al. (2006) Role of Sox2 in the development of the mouse neocortex. *Dev Biol* 295(1):52–66.
15. Park D, et al. (2009) The radial glia antibody RC2 recognizes a protein encoded by Nestin. *Biochem Biophys Res Commun* 382(3):588–592.
16. Misson JP, Edwards MA, Yamamoto M, Caviness VS, Jr (1988) Identification of radial glial cells within the developing murine central nervous system: Studies based upon a new immunohistochemical marker. *Brain Res Dev Brain Res* 44(1):95–108.
17. Gaiano N, Nye JS, Fishell G (2000) Radial glial identity is promoted by Notch1 signaling in the murine forebrain. *Neuron* 26(2):395–404.
18. Hartfuss E, Galli R, Heins N, Götz M (2001) Characterization of CNS precursor subtypes and radial glia. *Dev Biol* 229(1):15–30.
19. Shimada IS, Peterson BM, Spees JL (2010) Isolation of locally derived stem/progenitor cells from the peri-infarct area that do not migrate from the lateral ventricle after cortical stroke. *Stroke* 41(9):e552–e560.
20. Shimada IS, LeComte MD, Granger JC, Quinlan NJ, Spees JL (2012) Self-renewal and differentiation of reactive astrocyte-derived neural stem/progenitor cells isolated from the cortical peri-infarct area after stroke. *J Neurosci* 32(23):7926–7940.
21. Bard JD, et al. (2009) Signal transducer and activator of transcription 3 is a transcriptional factor regulating the gene expression of SALL4. *FASEB J* 23(5):1405–1414.
22. Ehret GB, et al. (2001) DNA binding specificity of different STAT proteins. Comparison of in vitro specificity with natural target sites. *J Biol Chem* 276(9):6675–6688.
23. Yokoyama S, Takeda K, Shibahara S (2006) SOX10, in combination with Sp1, regulates the endothelin receptor type B gene in human melanocyte lineage cells. *FEBS J* 273(8): 1805–1820.
24. Kamakura S, et al. (2004) Hes binding to STAT3 mediates crosstalk between Notch and JAK-STAT signalling. *Nat Cell Biol* 6(6):547–554.
25. Hamby ME, et al. (2012) Inflammatory mediators alter the astrocyte transcriptome and calcium signaling elicited by multiple G-protein-coupled receptors. *J Neurosci* 32(42):14489–14510.
26. Zamanian JL, et al. (2012) Genomic analysis of reactive astrogliosis. *J Neurosci* 32(18): 6391–6410.
27. Ge W, et al. (2002) Notch signaling promotes astrogliogenesis via direct CSL-mediated glial gene activation. *J Neurosci Res* 69(6):848–860.
28. Koyama Y, Michinaga S (2012) Regulations of astrocytic functions by endothelins: Roles in the pathophysiological responses of damaged brains. *J Pharmacol Sci* 118(4): 401–407.
29. Burda JE, Sofroniew MV (2014) Reactive gliosis and the multicellular response to CNS damage and disease. *Neuron* 81(2):229–248.
30. MacCumber MW, Ross CA, Snyder SH (1990) Endothelin in brain: Receptors, mitogenesis, and biosynthesis in glial cells. *Proc Natl Acad Sci USA* 87(6):2359–2363.
31. Paolillo M, Russo MA, Curti D, Lanni C, Schinelli S (2010) Endothelin B receptor antagonists block proliferation and induce apoptosis in glioma cells. *Pharmacol Res* 61(4):306–315.
32. Michinaga S, Ishida A, Takeuchi R, Koyama Y (2013) Endothelin-1 stimulates cyclin D1 expression in rat cultured astrocytes via activation of Sp1. *Neurochem Int* 63(1):25–34.
33. Koyama Y, et al. (1999) BQ788, an endothelin ET(B) receptor antagonist, attenuates stab wound injury-induced reactive astrocytes in rat brain. *Glia* 26(3):268–271.
34. Gadea A, Schinelli S, Gallo V (2008) Endothelin-1 regulates astrocyte proliferation and reactive gliosis via a JNK/c-Jun signaling pathway. *J Neurosci* 28(10):2394–2408.
35. Egnaczyk GF, et al. (2003) Proteomic analysis of the reactive phenotype of astrocytes following endothelin-1 exposure. *Proteomics* 3(5):689–698.
36. Lee JH, et al. (2009) Notch signal activates hypoxia pathway through HES1-dependent SRC/signal transducers and activators of transcription 3 pathway. *Mol Cancer Res* 7(10):1663–1671.
37. Fan X, et al. (2010) NOTCH pathway blockade depletes CD133-positive glioblastoma cells and inhibits growth of tumor neurospheres and xenografts. *Stem Cells* 28(1): 5–16.
38. Liu Y, et al. (2011) Autocrine endothelin-3/endothelin receptor B signaling maintains cellular and molecular properties of glioblastoma stem cells. *Mol Cancer Res* 9(12): 1668–1685.
39. Wan X, Zhang L, Jiang B (2014) Role of endothelin B receptor in oligodendroglioma proliferation and survival: In vitro and in vivo evidence. *Mol Med Rep* 9(1):229–234.
40. Committee on Care and Use of Laboratory Animals (1996) *Guide for the Care and Use of Laboratory Animals* (Natl Inst Health, Bethesda), DHHS Publ No (NIH) 85-23.
41. Chow LM, Zhang J, Baker SJ (2008) Inducible Cre recombinase activity in mouse mature astrocytes and adult neural precursor cells. *Transgenic Res* 17(5):919–928.
42. Carey BW, et al. (2009) Reprogramming of murine and human somatic cells using a single polycistronic vector. *Proc Natl Acad Sci USA* 106(1):157–162.
43. Tharp WG, et al. (2012) Measurement of altered AβPP isoform expression in frontal cortex of patients with Alzheimer's disease by absolute quantification real-time PCR. *J Alzheimers Dis* 29(2):449–457.
44. Livak KJ, Schmittgen TD (2001) Analysis of relative gene expression data using real-time quantitative PCR and the 2(-Delta Delta C(T)) Method. *Methods* 25(4):402–408.